



# A multicenter study of cervical cancer using quantitative diffusion-weighted imaging

Acta Radiologica  
2024, Vol. 65(7) 851–859  
© The Author(s) 2024



Article reuse guidelines:  
sagepub.com/journals-permissions  
DOI: 10.1177/02841851231222360  
journals.sagepub.com/home/acr



Xue Wang<sup>1,\*</sup> , Zhijun Ye<sup>2,\*</sup>, Shujian Li<sup>3,\*</sup>, Zhihan Yan<sup>1</sup>,  
Jingliang Cheng<sup>3</sup>, Gang Ning<sup>2</sup> and Zujun Hou<sup>1,4</sup> 

## Abstract

**Background:** Parameters from diffusion-weighted imaging (DWI) have been increasingly used as imaging biomarkers for the diagnosis and monitoring of treatment responses in cancer. The consistency of DWI measurements across different centers remains uncertain, which limits the widespread use of quantitative DWI in clinical settings.

**Purpose:** To investigate the consistency of quantitative metrics derived from DWI between different scanners in a multi-center clinical setting.

**Material and Methods:** A total of 193 patients with cervical cancer from four scanners (MRI1, MRI2, MRI3, and MRI4) at three centers were included in this retrospective study. DWI data were processed using the mono-exponential and intravoxel incoherent motion (IVIM) model, yielding the following parameters: apparent diffusion coefficient (ADC); true diffusion coefficient (D); pseudo-diffusion coefficient (D\*); perfusion fraction (f); and the product of f and D\* (fD\*). Various parameters of cervical cancer obtained from different scanners were compared.

**Results:** The parameters D and ADC derived from MRI1 and MRI2 were significantly different from those derived from MRI3 or MRI4 ( $P < 0.01$  for all comparisons). However, there was no significant difference in cervical cancer perfusion parameters (D\* and fD\*) between the different scanners ( $P > 0.05$ ). The  $P$  values of comparisons of all DWI parameters (D, D\*, fD\*, and ADC) between MRI3 and MRI4 (same vendor in different centers) for cervical cancer were all  $> 0.05$ , except for f ( $P = 0.05$ ).

**Conclusion:** Scanners of the same model by the same vendor can yield close measurements of the ADC and IVIM parameters. The perfusion parameters showed higher consistency among the different scanners.

## Keywords

Quantitative imaging, diffusion-weighted imaging, multicenter study, cervical cancer

Date received: 22 August 2023; accepted: 30 November 2023

## Introduction

Quantitative diffusion-weighted imaging (DWI) is an advanced magnetic resonance imaging (MRI) technique that has shown great potential for improving the biological characterization of cancer, and is increasingly being incorporated into clinical MRI protocols to assist in the differential diagnosis and therapeutic efficacy assessment of lesions (1–10). Popular metrics in quantitative DWI include the apparent diffusion coefficient (ADC) and parameters derived from the intravoxel incoherent motion model (IVIM) (11–13). To utilize such metrics as reliable biomarkers, it is imperative to understand the underlying variability of measurement, which generally depends on the

<sup>1</sup>Department of Radiology, The Second Affiliated Hospital and Yuying Children's Hospital of Wenzhou Medical University, Wenzhou, PR China

<sup>2</sup>Department of Radiology, The Second Affiliated Hospital of Sichuan University, Chengdu, PR China

<sup>3</sup>Department of MRI, The First Affiliated Hospital of Zhengzhou University, Zhengzhou, PR China

<sup>4</sup>Chinese Academy of Sciences, Suzhou Institute of Biomedical Engineering and Technology, Suzhou, PR China

\*Co-first authors, contributed equally, in data acquisition, data processing, literature study, manuscript drafting.

## Corresponding author:

Zujun Hou, Suzhou Institute of Biomedical Engineering and Technology, Chinese Academy of Sciences, 88 Keling Road, Huqiu District, Suzhou 215000, PR China.

Email: houzi@sibet.ac.cn

scanner platform, analysis method, and post-processing software (3,4,6,7,14–22).

Several studies have been conducted on the repeatability and reproducibility of quantitative DWI measurements (3,4,7,19–21). The test–retest repeatability of ADC measurements was evaluated in 23 patients with lung cancer examined in four institutions (three MRI vendors), and satisfactory repeatability and robustness to changes in postprocessing software have been reported (20). However, the study by Ghosh et al. showed that there was a statistically significant difference in the absolute ADC values obtained using different postprocessing software (21). Newitt et al. evaluated the repeatability and reproducibility of breast tumor ADC in a cohort of 89 women from nine institutions undergoing neoadjuvant chemotherapy for invasive breast cancer and concluded that breast tumor ADC could be measured with excellent repeatability and reproducibility in a multi-institution setting using a standardized protocol (19). However, these studies did not address the measurement variability between scanners.

Kivrak et al. compared ADC values among six 1.5-T MRI scanners from different vendors using a custom-made phantom solution consisting of distilled water and found that ADC values might differ among different MRI systems (15). Kolff-Gart et al. investigated the reproducibility of ADC values in the head and neck region by studying seven healthy individuals on five MRI scanners with echo-planar imaging (EPI) and turbo spin-echo (TSE) sequences and found that ADC values were more precise if individuals were measured on the same MRI system with the same sequence and that ADC values differed significantly between MRI systems and sequences (16). Nevertheless, these studies were performed using phantoms or only a small number of healthy volunteers without lesions with diffusion anomalies, and the findings might not be applicable to patients with cancer.

The consistency of quantitative DWI measurements across different centers remains uncertain, limiting the widespread use of quantitative DWI in clinical settings. The aim of the present study was to investigate the differences in ADC and IVIM parameters in patients with cervical cancer, as measured in a multicenter clinical setting using MRI scanners from different vendors.

## Material and Methods

### Study population

This retrospective study was approved by the local ethics review boards of the participating institutions. A total of 283 consecutive female patients who were diagnosed with cervical carcinoma by surgical pathology or biopsy and underwent MRI examination at one of the three centers between April 2016 and May 2021 were reviewed in this study. The inclusion criteria were as follows: (i) clinical

symptoms and cervical carcinoma diagnosed by histological examination; (ii) no history of chemoradiotherapy or surgery before MRI examination; and (iii) acceptable quality of MR images. Patients were excluded for the following reasons: (i) poor image quality of DWI, such as significant motion artifacts or incomplete images ( $n = 30$ ); (ii) history of targeted chemotherapy or radiation therapy before examination ( $n = 20$ ); (iii) history of biopsy before examination ( $n = 5$ ); and (iv) diagnosis of other cervical lesions, such as submucosal leiomyoma ( $n = 15$ ) of the uterus and endometrial carcinoma ( $n = 20$ ).

**Imaging protocol.** All MRI examinations were performed using one of the following scanners at the participating centers: a 3-T General Electric scanner (Discovery 750; GE Healthcare, Waukesha, WI, USA) at center 1; a 1.5-T Philips scanner (Achieva; Philips Healthcare, Best, The Netherlands) and a 3-T Siemens scanner (Skyra; Siemens AG, Erlangen, Germany) at center 2; and a 3-T Siemens scanner (Skyra; Siemens AG, Erlangen, Germany) at center 3, which were denoted as MRI1, MRI2, MRI3, and MRI4, respectively. Routine clinical images comprising T1-, T2-, and diffusion-weighted images were acquired. The parameter settings of the DWI protocols implemented using the different scanners are listed in Table 1.

### Image processing

Region-of-interest (ROI) delineation was performed on consecutive DWI slices independently by two experienced observers (with 13 and 15 years of experience) with reference to routine clinical scans (Fig. 1a). The size of the ROI was not less than 10 voxels to ensure robustness of the measurement. Areas of necrosis, cysts, and hemorrhages were avoided when drawing the lesion ROIs. Observers were blinded to the histopathological results. After manual delineation of all the datasets, each case was read by both observers to ensure high-quality measurements. Different opinions were resolved by consensus with a third observer when necessary. To reduce the impact of the differences in b-values on the measured quantitative DWI metrics, small b-values (10, 20, and 150  $\text{s/mm}^2$ ) and large b-values (1500  $\text{s/mm}^2$ ) were not included in the calculation.

DW images were analyzed using computer-aided software for DWI data analytics (MIalytics; FITPU Healthcare, Singapore). The following DWI parameters were derived: ADC from a mono-exponential model; diffusion coefficient (D); pseudo-diffusion coefficient ( $D^*$ ); perfusion fraction (f); and  $fD^*$  from IVIM. Representative parameter maps are shown in Fig. 1b–f.

ADC was calculated by fitting a mono-exponential model with all b-values  $\leq 1000 \text{ s/mm}^2$ .

$$\frac{S_b}{S_0} = \exp(-bD)$$

**Table 1.** Parameter setting of DWI protocol in different MRI scanners.

	MRI1	MRI2	MRI3	MRI4
Vendor	GE	Philips	Siemens	Siemens
Model	Discovery 750	Achieva	Skyra	Skyra
Field strength (T)	3.0	1.5	3.0	3.0
DWI protocol				
TE (ms)	74	66	58	85
TR (ms)	2400	3000	4100	4800
Percent phase	80	79	80	100
FOV (%)				
Matrix	192 × 160	116 × 116	140 × 112	128 × 109
Slice thickness (mm)	5	5	5	5
No. of b-values	6	6	9	12
b-value (s/mm <sup>2</sup> )	0, 30, 100, 200, 400, 1000	0, 50, 100, 200, 400, 1000	0, 10, 30, 50, 100, 150, 200, 400, 1000	0, 10, 20, 30, 50, 70, 100, 150, 200, 400, 800, 1500

DWI, diffusion-weighted imaging; FOV, field of view; MRI, magnetic resonance imaging; TE, echo time; TR, rotation time.

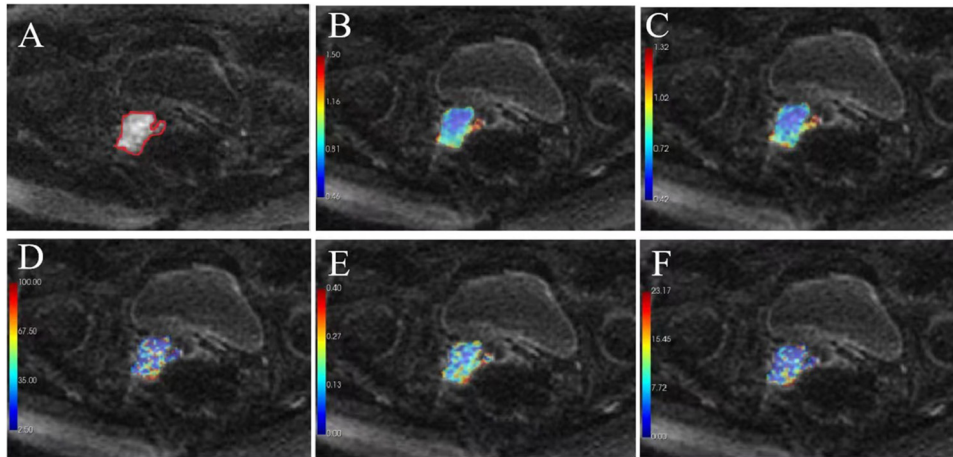


**Fig. 1.** The DWI ( $b = 1000 \text{ s/mm}^2$ ) of a 50-year-old woman with stage III cervix cancer (grade 3) as scanned using MRI1. (a) The ROI of cervix cancer (red circular) was manually drawn on each consecutive slice. (b) ADC map from a mono-exponential model. (c–f) diffusion coefficient (D), pseudodiffusion coefficient ( $D^*$ ), perfusion fraction (f), and  $fD^*$  maps from IVIM. ADC, apparent diffusion coefficient; DWI, diffusion-weighted imaging; IVIM, intravoxel incoherent motion; ROI, region of interest.

where  $S_b$  is the signal intensity of diffusion weighting  $b$ .

IVIM is given by:

$$\frac{S_b}{S_0} = (1 - f)\exp(-bD) + f\exp(-b(D^* + D))$$

where  $D$  is the diffusion coefficient associated with water diffusion in the extravascular space,  $D^*$  is the pseudo-diffusion coefficient related to perfusion in the vascular space, and  $f$  is the perfusion fraction. Thus, IVIM simultaneously estimates both diffusion ( $D$ ) and perfusion parameters ( $D^*$  and  $f$ ). Considering that  $D^*$  is markedly larger than  $D$ , the above equation is dominated by a mono-exponential function involving only  $D$  at  $b$  values  $\geq 200 \text{ s/mm}^2$ . A segmented two-step approach for estimating the IVIM parameters proposed by (1) was implemented,

where  $D$  was calculated by mono-exponentially fitting the signal intensities at  $b$ -values  $> 200 \text{ s/mm}^2$ . Then, with a fixed value of  $D$ ,  $D^*$  and  $f$  were estimated by fitting the signal intensities at all  $b$ -values  $\leq 1000 \text{ s/mm}^2$  in the bi-exponential function.

### Statistical analysis

Voxels in the ROIs of all slices from each patient were pooled together, and the median parameter value was taken as the representative value. DWI parameters ( $D$ ,  $f$ ,  $D^*$ ,  $fD^*$ , ADC) of cervical cancer in the three clinical centers showed uneven variances by homogeneity test of variance; therefore, the Kruskal–Wallis univariate ANOVA ( $K$  samples) method was used to compare various parameters in different centers.

Box plots were used to visualize the differences in the distribution of the corresponding parameter measurements at different centers. To reduce the impact of differences in patient demographics between samples, further comparisons were conducted between the scanners using cervical cancer data with the same degree of differentiation. The Mann–Whitney *U* test was performed to assess the differences in DWI parameters of moderately differentiated cervical cancer between MRI1 and MRI4 and DWI parameters of low-differentiated cervical cancer between MRI2 and MRI3. Coefficient of variation (CoV) was computed to measure the degree of reproducibility.  $P < 0.05$  indicated statistical significance. Statistical analyses were performed using SPSS version 21.0 (IBM Corp., Armonk, NY, USA).

## Results

### Study population

Of the 283 cases, 193 met the inclusion criteria and formed the final study cohort with a mean age of 55.2 years (age range = 35–75 years), 48.4 years (age range = 31–72 years), 48 years (age range = 31–75 years), and 52.1 years (age range = 33–72 years) in MRI1, MRI2, MRI3, and MRI4, respectively (Fig. 2). Patient characteristics are summarized in Table 2.

### Inter-scanner comparison on DWI parameters (*D*, *f*, *D*<sup>\*</sup>, *fD*<sup>\*</sup>, *ADC*)

The measured values of the DWI parameters (*D*, *f*, *D*<sup>\*</sup>, *fD*<sup>\*</sup>, and *ADC*) in cervical carcinoma were obtained. The distributions of DWI parameters were visualized

using box plots and are shown in Fig. 3 for cervical cancer tissue, where the differences among various parameters in different centers were assessed by Kruskal–Wallis univariate ANOVA (*K* samples), as indicated by the *P* values. The *P* values of comparisons of all DWI parameters (*D*, *D*<sup>\*</sup>, *fD*<sup>\*</sup>, and *ADC*) between MRI3 and MRI4 in cervical cancer tissue were all  $> 0.05$ , except for *f* ( $P = 0.05$ ), indicating that there was no significant difference in the measurements by these two MRI scanners. In contrast, when comparing the values of parameters *D*, *f*, and *ADC* derived from MRI2 with those derived from MRI3 or MRI4, the differences were significant ( $P < 0.01$  for all comparisons). Similarly, the measured values of parameter *D* and *ADC* from MRI1 in cervical cancer tissues were significantly different from those of MRI3 and MRI4 ( $P < 0.01$  for all comparisons). However, there was no significant difference in all cervical cancer perfusion parameters (*D*<sup>\*</sup>, *fD*<sup>\*</sup>) between different scanners from different centers ( $P > 0.05$ ) (Table 3).

### Inter-scanner comparison on DWI parameters in the same grade of cervical cancer

In the above comparison, the findings could be affected by the differences in patient demographics associated with different scanners. To reduce this effect, further comparisons were performed using the cervical cancer data with the same degree of differentiation. MRI3 and MRI4 are the same type of scanner from the same manufacturer, and DWI parameters (*D*, *f*, *D*<sup>\*</sup>, *fD*<sup>\*</sup>, *ADC*) from these two scanners showed no significant differences ( $P > 0.05$ ); hence, data from these two scanners were combined and explored for differences with respect to MRI1 in grade 2 cervical

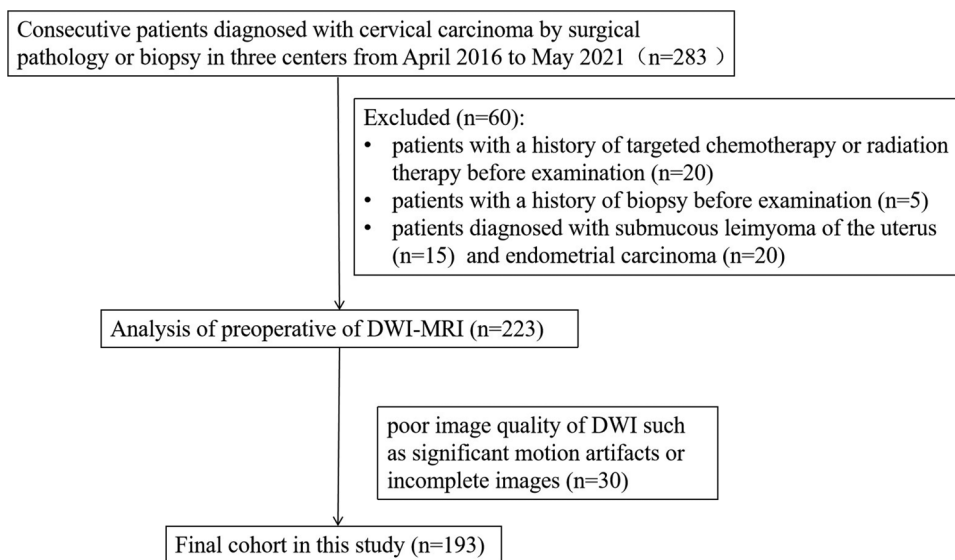


Fig. 2. Flow chart of patient population.

**Table 2.** Patient demography of this study.

Characteristics	MRI1 (n = 58)	MRI2 (n = 55)	MRI3 (n = 27)	MRI4 (n = 53)
Age (years)	55.2 (35–75)	48.4 (31–72)	48.0 (31–75)	52.1 (33–72)
Histologic type				
SCC	56	45	20	46
Adenocarcinoma	2	7	4	4
Adenosquamous carcinoma	0	3	3	3
Grade				
G1	14	3	3	2
G2	23	5	5	26
G3	3	35	15	11
Not graded	18	12	4	14
Clinic stage				
I a	6	6	2	0
I b	23	36	15	13
II a	15	8	5	19
II b	7	3	3	5
III a	4	2	2	2
III c	2	0	0	10
IV a	1	0	0	3
IV b	0	0	0	1
Treatment before MR examination				
Chemoradiotherapy	0	0	0	0
Surgery	0	0	0	0

Values are given as n or median (range).

DWI, diffusion-weighted imaging; MRI, magnetic resonance imaging; SCC, squamous cell carcinoma.

**Table 3.** Inter-scanner comparison of DWI parameters (*P* values) using the Kruskal–Wallis ANOVA test.

	D ( $10^3\text{mm}^2/\text{s}$ )	F	D* ( $10^3\text{mm}^2/\text{s}$ )	fD* ( $10^{-3}\text{mm}^2/\text{s}$ )	ADC ( $10^{-3}\text{mm}^2/\text{s}$ )
Kruskal–Wallis ANOVA	<0.001	<0.001	0.557	0.157	<0.001
MRI1–MRI2	0.332	<0.001	-	-	0.598
MRI1–MRI3	0.003	0.207	-	-	<0.001
MRI1–MRI4	<0.001	0.351	-	-	<0.001
MRI2–MRI3	<0.001	<0.001	-	-	0.001
MRI2–MRI4	<0.001	0.003	-	-	<0.001
MRI3–MRI4	0.380	0.05	-	-	0.099

ADC, apparent diffusion coefficient; ANOVA, analysis of variance; DWI, diffusion-weighted imaging; MRI, magnetic resonance imaging.

cancer and the difference with MRI2 in grade 3 cervical cancer. The measured values of DWI parameters (D, f, D\*, fD\*, and ADC) in these grades of cervical cancer tissue from the respective scanners are summarized in Table 4, where the Mann–Whitney *U* test results and coefficients of variation are also presented. It can be observed that the values were significantly different in both grade 2 and grade 3 cervical cancer groups ( $P < 0.001$ ). The difference in parameter D was significant in grade 3 cervical cancer ( $P < 0.001$ ), but not in grade 2 cervical cancer ( $P = 0.107$ ). There were no significant differences in any of the perfusion parameters (f, D\*, and fD\*) ( $P > 0.2$ ). CoV was comparatively larger in ADC than in IVIM. The box plots

in Fig. 4 show the distributions of ADC and IVIM parameters in these comparisons.

## Discussion

This study investigated the differences in ADC and IVIM parameters in patients with cervical cancer measured independently using MRI scanners from different vendors, which has rarely been reported in the literature but is important for the adoption of this technique in clinical practice. The results showed that scanners of the same model by the same vendor (MRI3 vs. MRI4) could yield close measurements of

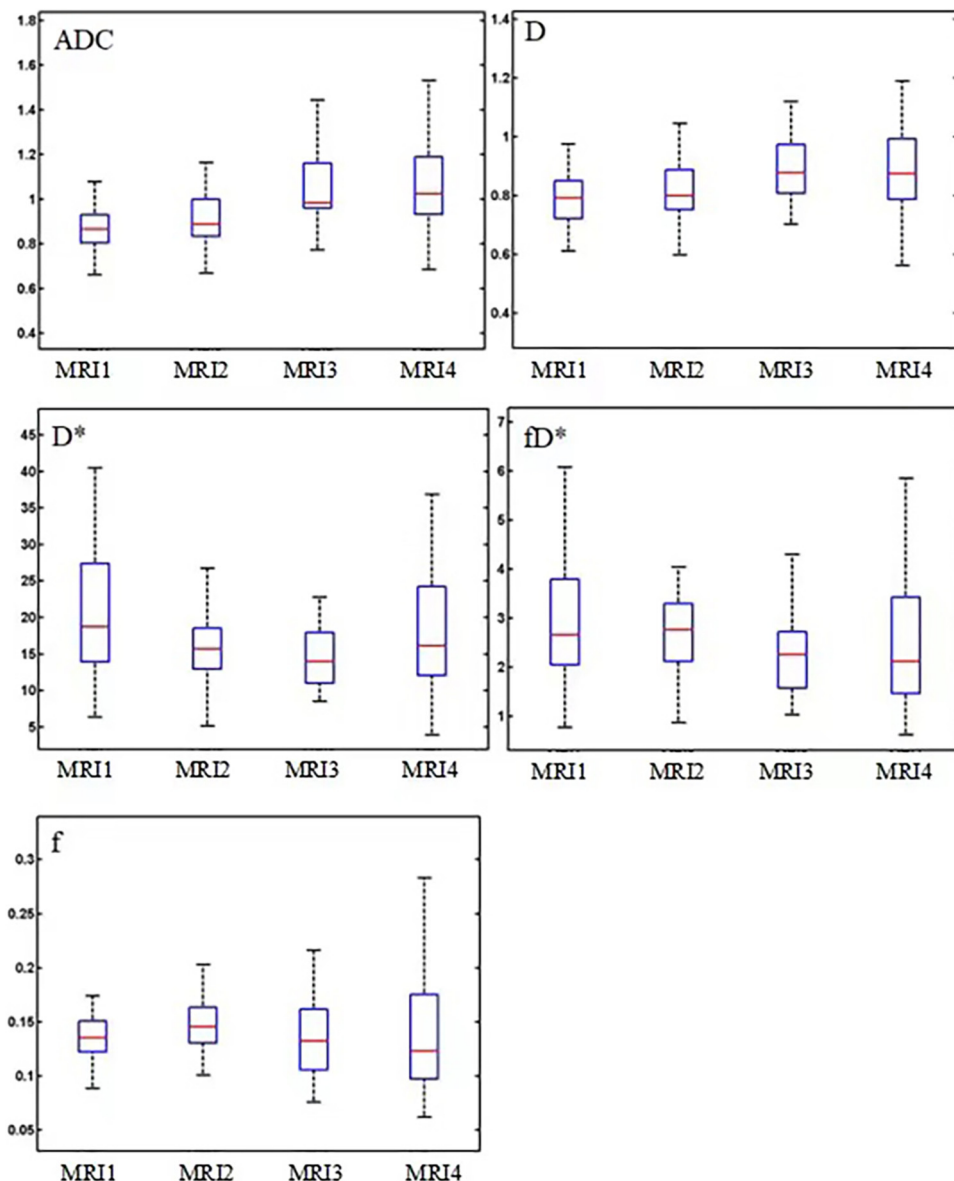


**Fig. 3.** Box plots of the distributions of DWI parameter (ADC, D, f, D\*, fD\*) measurements of cervical cancer tissue using four MRI scanners (GE 750, Philips Achieva, Siemens Skyra, and Siemens Skyra) from three centers. ADC, apparent diffusion coefficient; DWI, diffusion-weighted imaging; MRI, magnetic resonance imaging.

ADC and IVIM parameters, and perfusion parameters attained higher consistency among all the different scanners.

The values of ADC and D differed significantly between scanners from different vendors in cervical cancer tissue ( $P < 0.01$  for all comparisons) except for ADC and D between GE 750 and Philips Achieva ( $P = 0.598$  and  $0.332$ , respectively) and D in grade 2 cervical cancer between GE 750 and Siemens Skyra ( $P = 0.107$ ). This finding was in agreement with the results in previous studies (15,16), where ADC values were more precise if individuals were measured on the same MR system with the same sequence, and that ADC values differed significantly between MR systems and sequences. A possible explanation for this result is as

follows: even when acquisition and analysis methods are standardized between centers, differences remain in the imaging settings of gradient pulses between the MR scanners. In quantitative DWI, the diffusion gradients were characterized using the b-value.

$$b = q^2 \left( \Delta - \frac{\delta}{3} \right)$$

where  $q^2$  describes the gradient pulses and depends on the amplitude  $G$ , duration of diffusion gradients  $\delta$ , time interval between diffusion-sensitizing gradients  $\Delta$ , and  $t_D = (\Delta - \delta/3)$  represents the diffusion time. Evidently, the same b-value does not imply that the diffusion time and

**Table 4.** Measured values of DWI parameters in different grades of cervical cancer tissue from various scanners, the results of Mann-Whitney *U* test and CoV.

	D ( $10^{-3}\text{mm}^2/\text{s}$ )	F	D* ( $10^{-3}\text{mm}^2/\text{s}$ )	fD* ( $10^{-3}\text{mm}^2/\text{s}$ )	ADC ( $10^{-3}\text{mm}^2/\text{s}$ )
<b>Grade 2</b>					
MRI1 (n = 23)	0.85 ± 0.08	0.14 ± 0.04	21.74 ± 10.51	3.27 ± 1.95	0.92 ± 0.08
MRI3 + MRI4 (n = 31)	0.95 ± 1.18	0.15 ± 0.07	26.19 ± 18.11	4.04 ± 3.58	1.13 ± 0.25
P value	0.107	0.826	0.733	0.922	<0.001
CoV (%)	3.2	4.5	4.1	6.0	7.9
<b>Grade 3</b>					
MRI2 (n = 35)	0.80 ± 0.11	0.15 ± 0.02	17.56 ± 6.66	2.92 ± 1.02	0.88 ± 0.12
MRI3 + MRI4 (n = 26)	0.95 ± 0.20	0.14 ± 0.06	21.94 ± 19.57	3.24 ± 2.73	1.12 ± 0.29
P value	<0.001	0.208	0.680	0.310	<0.001
CoV (%)	7.3	6.4	2.0	10.4	11.2

Values are given as mean ± SD unless otherwise indicated.

CoV, coefficient of variation; DWI, diffusion-weighted imaging; MRI, magnetic resonance imaging; SD, standard deviation.

gradient pulses are the same. In DWI settings,  $\Delta$  can be adjusted with a corresponding change in the G value such that b and  $\delta$  remain constant (23). It was found that only a slight change in the signal intensity of normal tissue was observed with a longer interval  $\Delta$  and the same b-value; however, the signal intensity of tissue with restricted diffusion in tumor tissue increased by 140% (24), indicating that DWI signals are specifically  $\Delta$ -dependent in tumor tissue, which could be overlooked by test-retest scans in studies using phantoms or volunteers. This might account for the significant differences in the ADC and D measurements of cervical cancer tissue between scanners from different vendors, as observed in this study. It should be noted that the values of ADC and IVIM parameters of cervical cancer tissue between Siemens Skyra of center 2 and Siemens Skyra of center 3 were similar ( $P > 0.05$ ), which could be because both scanners were the same model from the same vendor and hence had similar gradient pulses and imaging settings.

A critical review of the variety of acquisition and analysis methodologies in ADC employed at different centers was provided in a previous study by deSouza et al. (25). The ADC values were hardly comparable between centers, which limits the utility of ADC as a biomarker and casts doubt on the favorable results of multicenter trials using ADC. DeSouza et al. (25) discussed hardware and software considerations when implementing standardized protocols across multivendor platforms, together with methods for quality assurance and quality control, and proposed building an international consensus on procedures for successful validation of ADC. Based on the present study, it is essential for vendors to have a consensus on gradient pulses and other imaging settings for the implementation of quantitative DWI.

Alternatively, it is crucial to develop more precise diffusion models to analyze the quantitative DWI data. Common diffusion models for DWI are based on the

Stejskal-Tanner pulse sequence, assuming no restriction on diffusion, and describe the diffusion of water molecules in tissue using a Gaussian distribution, leading to an exponential decay of the DWI signal intensity with respect to the b-value. However, the physical mode of diffusion in tissues is complicated by the variety of tissue microstructures and presence of other transport processes. Diffusion can be restricted within a confined space (such as cells) or hindered in the extracellular space. The signal can also be affected by blood perfusion or water exchange between cell membranes. As shown in the study by Hope et al. (24), both the primary tumor site with high cell density and the intermediate region with intermediate cell density demonstrated a strong dependence on  $\Delta$ , whereas the b-value was fixed, illustrating the non-Gaussian distribution of water molecule diffusion in cancer tissue. Although models have been proposed to address this non-Gaussian issue, such as stretched exponential (26), kurtosis imaging (27), and restriction spectrum imaging (28), limited efforts have considered the impact of imaging gradient pulses or other imaging settings on the modeling of quantitative DWI data (24).

It is interesting to note that IVIM perfusion parameters tended to show higher consistency between scanners than ADC and D (Table 4). No significant difference was observed in the cervical cancer perfusion parameters (D\*, fD\*) between different scanners from different centers ( $P > 0.05$ ). Comparatively, the consistency between scanners for another perfusion parameter (f) varied from  $P < 0.01$  to  $P > 0.05$ , which could result from the impact of estimation of D on f, because f essentially weighs the different contributions from the true diffusion of water molecules and the pseudo-diffusion from blood flow. The IVIM is a special form of the bi-exponential model that differentiates pseudo-diffusion due to blood microcirculation in the capillary network from the true diffusion of water molecules in the tissue.

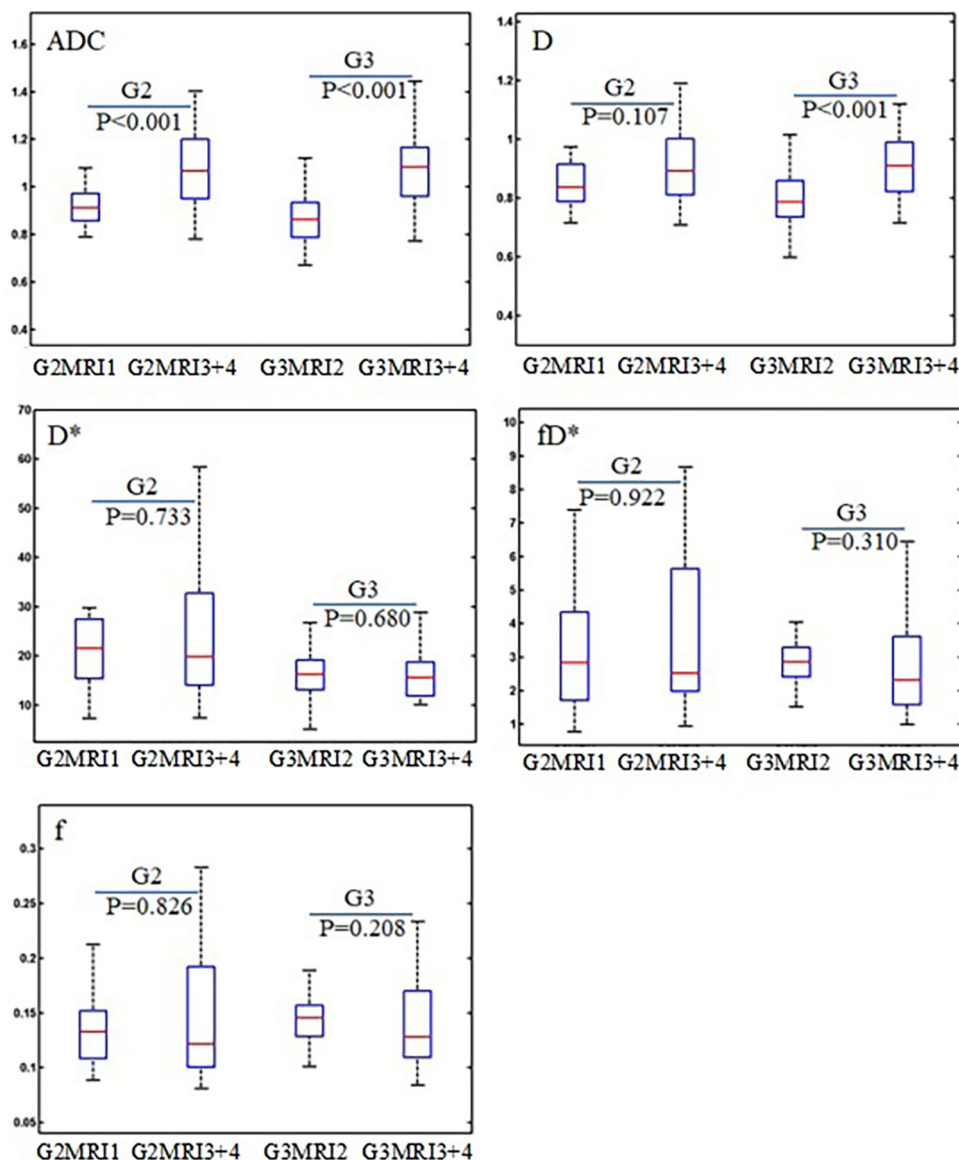


**Fig. 4.** Box plots of DWI parameter (ADC, D, f, D\*, fD\*) measurements of cervical cancer tissue between MRI scanners with the same grade of cervical cancer (GE 750 vs. Siemens Skyra for G2; Philips Achieva vs. Siemens Skyra for G3), where G2 stands for grade 2 and G3 for grade 3. P values indicated the results of the Mann–Whitney U test. ADC, apparent diffusion coefficient; DWI, diffusion-weighted imaging; MRI, magnetic resonance imaging.

The observed higher consistency of perfusion parameters between the scanners suggests that the estimation of these parameters was less affected by the diffusion gradient pulses, which could shed light on the development of more advanced diffusion models in the future.

The present study has some limitations. Compared to phantom studies or repeated scans of volunteers, using patient data scanned independently is prone to variations in patient characteristics. This issue was addressed in this study by comparing subsets of patient data from the same grade. Nevertheless, the preliminary findings in the present study need to be further validated in a larger-

scale study where the samples collected by different scanners would be more balanced in terms of patient demography. It can be seen that with sufficiently large sample sizes, the findings would converge to those with repeated scans of patients.

In conclusion, the perfusion parameters from IVIM attained higher consistency between the scanners. The measured ADC and D values showed significant differences between the scanners of the different vendors. This difference could be due to the association of the diffusion signal and imaging gradient pulse settings, as well as the non-Gaussian distribution of water molecular diffusion in the tissue.



## Declaration of conflicting interests


The authors declared no potential conflicts of interest with respect to the research, authorship, and/or publication of this article.

## Funding

The authors disclosed receipt of the following financial support for the research, authorship, and/or publication of this article: This work was supported by the Wenzhou Science and Technology Bureau in China (No. Y20220070) and Zhejiang Provincial Medical and Health Project (No. 2023RC212).

## ORCID iDs

Xue Wang  <https://orcid.org/0000-0001-6178-6316>

Zujun Hou  <https://orcid.org/0000-0002-3354-7358>

## References

- Luciani A, Vignaud A, Cavet M, et al. Liver cirrhosis: intravoxel incoherent motion MR imaging—pilot study. *Radiology* 2008;249:891–899.
- White NS, McDonald C, Farid N, et al. Diffusion-weighted imaging in cancer: physical foundations and applications of restriction spectrum imaging. *Cancer Res* 2014;74:4638–4652.
- Bernardin L, Douglas NH, Collins DJ, et al. Diffusion-weighted magnetic resonance imaging for assessment of lung lesions: repeatability of the apparent diffusion coefficient measurement. *Eur Radiol* 2014;24:502–511.
- Ye XH, Gao JY, Yang ZH, et al. Apparent diffusion coefficient reproducibility of the pancreas measured at different MR scanners using diffusion-weighted imaging. *J Magn Reson Imaging* 2014;40:1375–1381.
- Partridge SC, Nissan N, Rahbar H, et al. Diffusion-weighted breast MRI: clinical applications and emerging techniques. *J Magn Reson Imaging* 2017;45:337–355.
- Mikayama R, Yabuuchi H, Sonoda S, et al. Comparison of intravoxel incoherent motion diffusion-weighted imaging between turbo spin-echo and echo-planar imaging of the head and neck. *Eur Radiol* 2018;28:316–324.
- Pan J, Zhang H, Man F, et al. Measurement and scan reproducibility of parameters of intravoxel incoherent motion in renal tumor and normal renal parenchyma: a preliminary research at 3.0 T MR. *Abdom Radiol* 2018;43:1739–1748.
- Tang L, Zhou XJ. Diffusion MRI of cancer: from low to high b-values. *J Magn Reson Imaging* 2019;49:23–40.
- Iima M, Honda M, Sigmund EE, et al. Diffusion MRI of the breast: current status and future directions. *J Magn Reson Imaging* 2020;52:70–90.
- Lecler A, Duron L, Zmuda M, et al. Intravoxel incoherent motion (IVIM) 3 T MRI for orbital lesion characterization. *Eur Radiol* 2021;31:14–23.
- Le Bihan D, Breton E, Lallemand D, et al. MR Imaging of intravoxel incoherent motions: application to diffusion and perfusion in neurologic disorders. *Radiology* 1986;161:401–407.
- Le Bihan D. Intravoxel, incoherent motion imaging using steady-state free precession. *Magn Reson Med* 1988;7:346–351.
- Koh DM, Collins DJ, Orton MR. Intravoxel incoherent motion in body diffusion-weighted MRI: reality and challenges. *AJR Am J Roentgenol* 2011;196:1351–1361.
- Ogura A, Hayakawa K, Miyati T, et al. Imaging parameter effects in apparent diffusion coefficient determination of magnetic resonance imaging. *Eur J Radiol* 2011;77:185–188.
- Kivrak AS, Paksoy Y, Erol C, et al. Comparison of apparent diffusion coefficient values among different MRI platforms: a multicenter phantom study. *Diagn Interv Radiol* 2013;19:433–437.
- Kolff-Gart AS, Pouwels PJ, Noij DP, et al. Diffusion-weighted imaging of the head and neck in healthy subjects: reproducibility of ADC values in different MRI systems and repeat sessions. *AJNR Am J Neuroradiol* 2015;36:384–390.
- Malyarenko D, Galbán CJ, Londy FJ, et al. Multi-system repeatability and reproducibility of apparent diffusion coefficient measurement using an ice-water phantom. *J Magn Reson Imaging* 2013;37:1238–1246.
- Sumikawa T, Yabuuchi H, Sumikawa C, et al. Influence of blade width and magnetic field strength on the ADC on PROPELLER DWI in head and neck. *Neuroradiol J* 2020;33:39–47.
- Newitt DC, Zhang Z, Gibbs JE, et al. Test-retest repeatability and reproducibility of ADC measures by breast DWI: results from the ACRIN 6698 trial. *J Magn Reson Imaging* 2019;49:1617–1628.
- Weller A, Papoutsaki MV, Waterton JC, et al. Diffusion-weighted (DW) MRI in lung cancers: ADC test-retest repeatability. *Eur Radiol* 2017;27:4552–4562.
- Ghosh A, Singh T, Singla V, et al. Comparison of absolute apparent diffusion coefficient (ADC) values in ADC maps generated across different postprocessing software: reproducibility in endometrial carcinoma. *AJR Am J Roentgenol* 2017;209:1312–1320.
- Malyarenko DI, Newitt D, Wilmes LJ, et al. Demonstration of nonlinearity bias in the measurement of the apparent diffusion coefficient in multicenter trials. *Magn Reson Med* 2016;75:1312–1323.
- Ferizi U, Schneider T, Witzel T, et al. White matter compartment models for in vivo diffusion MRI at 300 mT/m. *NeuroImage* 2015;118:468–483.
- Hope TR, White NS, Kuperman J, et al. Demonstration of non-Gaussian restricted diffusion in tumor cells using diffusion time-dependent diffusion-weighted magnetic resonance imaging contrast. *Front Oncol* 2016;6:179.
- deSouza NM, Winfield JM, Waterton JC, et al. Implementing diffusion-weighted MRI for body imaging in prospective multicenter trials: current considerations and future perspectives. *Eur Radiol* 2018;28:1118–1131.
- Bennett KM, Schmainda KM, Bennett RT, et al. Characterization of continuously distributed cortical water diffusion rates with a stretched-exponential model. *Magn Reson Med* 2003;50:727–734.
- Jensen JH, Helpert JA. Diffusional kurtosis imaging: the quantification of non-Gaussian water diffusion by means of magnetic resonance imaging. *Magn Reson Med* 2005;53:1432–1440.
- White NS, Leergaard TB, D'Arceuil H, et al. Probing tissue microstructure with restriction spectrum imaging: histological and theoretical validation. *Hum Brain Mapp* 2013;34:327–346.